

Calix[5]arene Through-the-Annulus Threading of Dialkylammonium Guests Weakly Paired to the TFPB Anion

Margherita De Rosa,^{,†} Carmen Talotta,[†] Carmine Gaeta,[†] Annunziata Soriente,[†] Placido Neri^{*,†}*

Sebastiano Pappalardo,[§] Giuseppe Gattuso,[‡] Anna Notti,[‡] Melchiorre F. Parisi,^{,‡} and Ilenia*

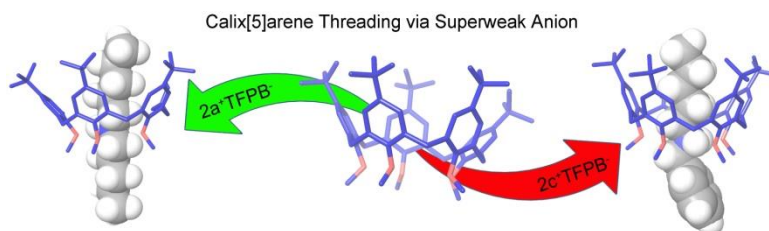
Pisagatti[‡]

[†]Dipartimento di Chimica e Biologia "A. Zambelli", Università di Salerno, Via Giovanni Paolo II 132, I-84084 Fisciano (Salerno), Italy, e-mail: maderosa@unisa.it, neri@unisa.it

[‡] Dipartimento di Scienze Chimiche, Biologiche, Farmaceutiche ed Ambientali, Università di Messina, Viale F. Stagno d'Alcontres 31, I-98166, Messina, Italy, e-mail: mparisi@unime.it

[§]Dipartimento di Scienze Chimiche, Università di Catania, Viale A. Doria 6, I-95125, Catania, Italy

RECEIVED DATE (to be automatically inserted after your manuscript is accepted if required according to the journal that you are submitting your paper to)



ABSTRACT. The *through-the-annulus* threading of calix[5]arene penta-O-ethers by dialkylammonium cations coupled to the loosely coordinating *superweak* TFPB[−] anion has been successfully accomplished. ¹H NMR titration data show that the preorganization of the calix[5]arene scaffold leads to great thermodynamic stability of the pseudorotaxane complexes as well as to a favorable kinetic of threading. Accordingly, calix[5]arene **1c**, bearing *tert*-butyl groups at the wide rim, was threaded by all the cations under study (with the exception of the dibenzylammonium **2b**⁺) more tightly than the other derivatives under investigation (K_{as} up to $2.02 \pm 0.2 \times 10^5 \text{ M}^{-1}$) because of its preorganized *cone* conformation. According to DFT calculations, van der Waals interactions between the *tert*-butyl groups of **1c** and the alkyl chain of the cationic axle are likely responsible for the remarkable stability observed. The threading of the calix[5]arene wheels with the asymmetric pentylbenzylammonium axle led to the toposelective formation of the *endo*-pentyl pseudorotaxane stereoisomer in agreement with the known “*endo*-alkyl rule”. Owing to the steric hindrance of the axle phenyl group, the threading of the guest was seen to occur in a unidirectional fashion through the calixarene narrow rim.

Introduction

Interpenetrated molecules such as rotaxanes and catenanes ¹ are attractive supramolecular architectures that may also behave as molecular machines ² or act as catalysts.³ Pseudorotaxanes are molecular assemblies obtained by the insertion of a rod-like guest inside a macrocyclic host molecule (threading) and, as such, can be considered as the precursors of rotaxanes and catenanes. ¹ Historically,

crown ethers⁴ were the first molecules to be used as wheel components for the assembly of interpenetrated structures followed, in the past two decades, by a number of different macrocycles including cyclodextrins,⁵ cucurbiturils,⁶ macrolactams,⁷ calixarenes⁸ and most recently pillararenes.⁹

With reference to calixarene-based interpenetrated systems, Arduini, Pochini and co-workers have extensively studied pseudorotaxanes/rotaxanes based on calix[6]arene macrocycles and viologen-derived linear axles,¹⁰ while some of us have mainly focused our attention on the threading of the calix[6]arene-wheel with dialkylammonium axles (e.g.: **2a–c**⁺).¹¹ In these studies, we have shown that di-*n*-alkylammonium cations are able to thread the calix[6]arene annulus only when they are coupled to the loosely coordinating Tetrakis[3,5-bis(triFluoromethyl)Phenyl]Borate (TFPB⁻) “superweak anion” (Chart 1).^{11a, 12}

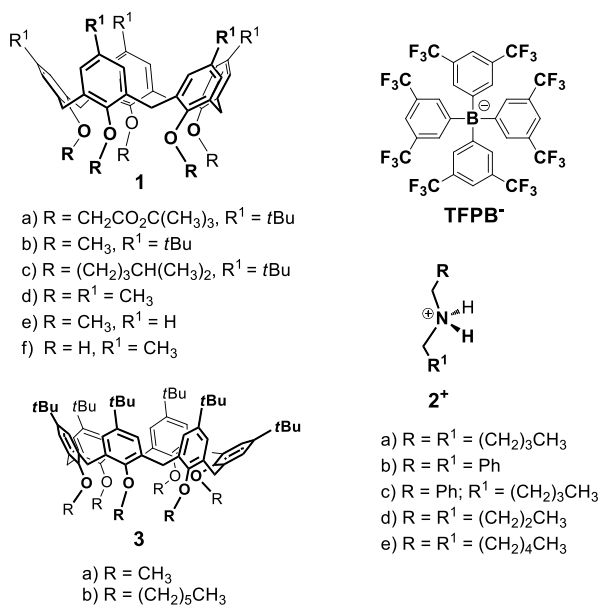


Chart 1. Structures of calix[5]arene derivatives **1a–f**, dialkyl ammonium **2a–e**⁺TFPB⁻ salts and calix[6]arene hosts **3a,b**.

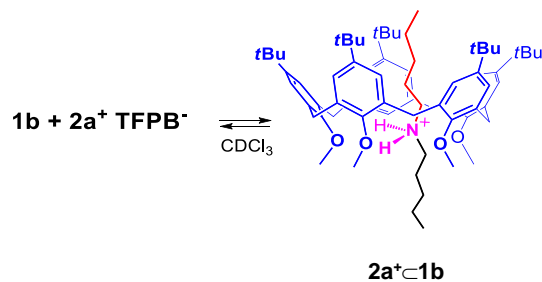
The threading abilities of dialkylammonium axles strongly depend on the size of the target calixarene macrocycle.¹³ Hence, no hint of threading was observed between dialkylammonium cations and larger calix[8]arene,^{13a} smaller calix[4]arene^{13b} or dihomooxalix[4]arene^{13c} macrocycles.

As for calix[5]arene-based pseudorotaxanes, only two examples of dialkylammonium axles **2d,e**⁺ (as Cl⁻, PF₆⁻, and picrate salts) threading through penta-*O*-ester **1a**¹⁴ have so far been reported.¹⁵ In these cases, the formation of additional hydrogen bonds between the ammonium ion and the carbonyl group(s) of the host molecule was postulated to play an important role in the formation of the **2d**⁺⊂**1a** pseudorotaxane.¹⁵ Conversely, no trace of threading was detected, by ¹H NMR spectroscopy, when penta-*O*-ethers **1b,c**, lacking the C=O groups, were mixed in CDCl₃ with the same axle salts.¹⁶

Thus, considering the effectiveness of the superweak anion approach in inducing the threading of secondary ammonium ions through the annulus of scarcely preorganized and/or narrow macrocyclic hosts,^{11,17} we decided to study the formation of calix[5]arene-based pseudorotaxanes in the presence of dialkylammonium TFPB salts.

Results and Discussion

Threading studies with the di-*n*-pentylammonium tetrakis[3,5-bis(trifluoromethyl)phenyl]borate (2a**⁺TFPB⁻) axle.** We initially investigated the threading of the conformationally mobile penta-*O*-methyl-*p*-*tert*-butylcalix[5]arene **1b**¹⁸ with the **2a**⁺TFPB⁻ salt. Derivative **1b**, owing to the small size of the methyl substituents present at the narrow rim, rapidly undergoes cone-to-cone interconversion (*OMe through-the-annulus passage*)¹⁹ and as a result it displays a ¹H NMR spectrum (in CDCl₃ at 298 K) with sharp signals (Figure 1a)²⁰ typical of a fast conformational mobility on the NMR timescale.^{18,19} However, upon addition of **2a**⁺TFPB⁻ to a CDCl₃ solution of **1b** a new set of signals consistent with the formation of pseudorotaxane **2a**⁺⊂**1b** was clearly observed (Scheme 1).



Scheme 1. Formation of the **2a⁺⊂1b** pseudorotaxane

The most evident of these are a well-defined AX system at $\delta = 4.28$ and 3.53 ppm ($J = 13.8$ Hz) for the ArCH₂Ar groups, indicative of a blocked *cone* conformation of the wheel **1b**, and four alkyl resonances in the upfield negative region of the spectrum (from -0.76 to -2.40 ppm), diagnostic of a shielded through-the-annulus threaded **2a⁺** axle. In agreement with the formation of the **2a⁺⊂1b** pseudorotaxane, close examination of the COSY-45 spectrum¹⁶ of a 1:1 mixture of **1b** and **2a⁺TFPB⁻** in CDCl₃, revealed the presence of two different axle pentyl chains: one hosted inside the cavity and, as a result, strongly shielded (with ϵ , δ , β , γ , and α hydrogen atoms resonating at $\delta = -0.77$, -0.86 , -1.76 , -2.36 and 1.71 ppm, respectively); the other protruding from the cavity in the direction of the narrow rim, most conspicuously showing a downfield shift for the α - and β -CH₂s ($\delta = 3.61$ and 1.98 ppm, respectively).

The threading of **1b** reached an equilibrium after 96 h (at 298 K) from the addition of **2a⁺**, with a percentage of formation of 50% and an apparent association constant (K_a) for the **2a⁺⊂1b** complex of 460 ± 50 M⁻¹, calculated by direct integration of appropriate signals of the threaded and unthreaded species (**2a⁺** or **1b**). As expected, the same equilibrium percentage was reached more rapidly (after 46 h) at 348 K.

Interestingly, the shielded pentyl hydrogen atoms of **2a⁺** experiencing the highest Complexation Induced Shift (CIS) are the γ and β ones, which undergo substantial upfield shifts ($\Delta\delta = 3.59$ and 3.25 ppm, respectively). The α -CH₂ in the **2a⁺⊂1b** calix[5]-pseudo[2]rotaxane experiences a CIS of 1.20 ppm, a value significantly lower than that observed for the analogous group in the **2a⁺⊂3a** calix[6]-

pseudo[2]rotaxane ($\Delta\delta = 2.31$ ppm).^{11a} These data suggest that in the former the $2a^+$ axle penetrates more deeply inside the cavity of **1b**, bringing the ammonium group closer to the oxygen mean plane and, at the same time, dragging the α -CH₂ away from the region of maximum shielding provided by the aromatic rings.

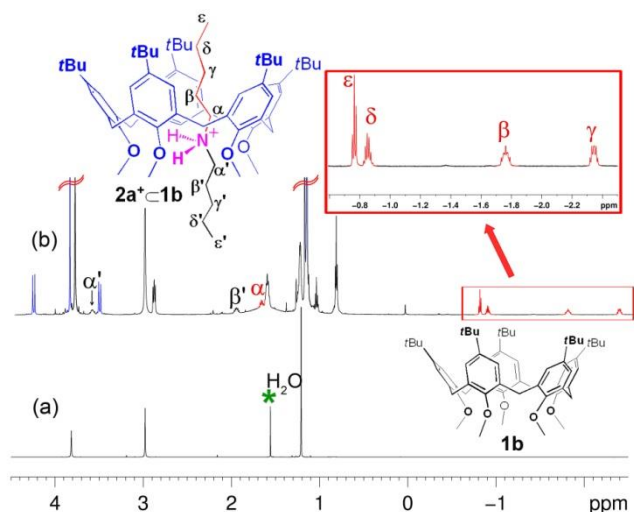


Figure 1. High-field regions of the ¹H NMR spectra (600 MHz, CDCl₃, 298 K) of: (a) **1b** and (b) an equimolar solution (4.5 mM) of **1b** and $2a^+$ TFPB⁻ after 46 h at 348 K.

This overall picture was confirmed by a close inspection of the DFT-optimized structure of $2a^+ \subset 1b$ (Figure 2) at the B3LYP/6-31G(d,p) level of theory, which revealed that the axle N-atom sits 0.30 Å above the phenolic oxygen atoms mean plane. This value is significantly lower with respect to that previously observed (0.53 Å) for the analogous calix[6]-pseudorotaxane.^{11a} The DFT-optimized structure of $2a^+ \subset 1b$ (Figure 2) displays the expected stabilizing intermolecular H-bonds between the ammonium group of $2a^+$ and the oxygen atoms of **1b** (average N⁺⋯O distance 2.75 Å). In addition, the pseudorotaxane complex takes advantage of CH⋯π¹⁶ and van der Waals interactions between the aryl rings and the *tert*-butyl groups at the wide rim of **1b**, respectively, and the *endo*-cavity included pentyl chain of $2a^+$ (Figures 2a–c).

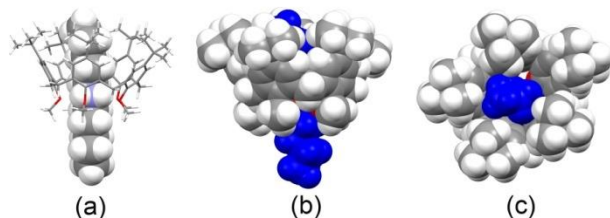


Figure 2. Different views of the optimized structure of the $2a^+ \subset 1b$ pseudo[2]rotaxane at the B3LYP/6-31G(d,p) level of theory.

The replacement of calix[5]arene **1b** with the highly preorganized, *cone*-shaped penta-*O*-(4-methylpentyl) derivative **1c**^{19, 21} (AX system at $\delta = 4.54$ and 3.25 ppm for the ArCH₂Ar group; see Figure 3a) was then considered, with the aim of evaluating the effect of a preorganized wheel on the axle threading process.

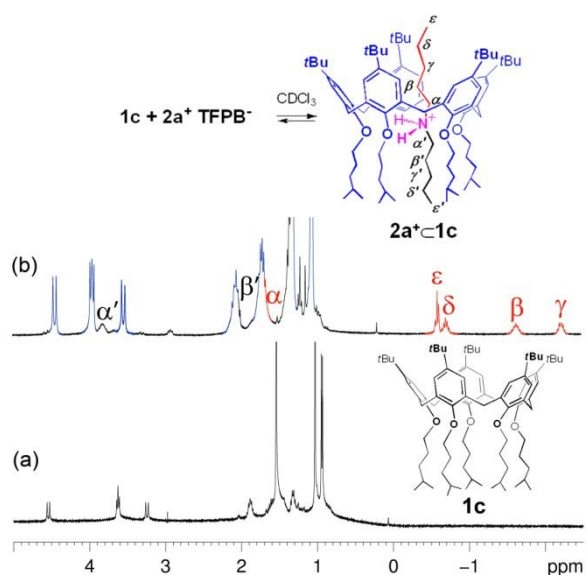


Figure 3. High-field regions of the ¹H NMR spectra (300 MHz, CDCl₃, 298 K) of: (a) **1c**, (b) an equimolar solution (4.5 mM) of **1c** and $2a^+TFPB^-$ after 18 h at rt.

Addition of an equimolar amount of $2a^+TFPB^-$ to a CDCl₃ solution of **1c**, gave rise to a ¹H NMR spectrum fully consistent with the formation of the $2a^+ \subset 1c$ pseudorotaxane (Figure 3). At room

temperature, the complexation equilibrium of $2a^+ \subset 1c$ was reached faster (18 h) than in the case of the analogous pseudorotaxane $2a^+ \subset 1b$ (96 h).

Calculation of the apparent association constant of the pseudorotaxane –by direct peak integration– was not satisfactory as the intensities of the 1H NMR signals (Figure 3b) of the host $1c$ and guest $2a^+$ in the unbound forms were found to be below (about 8%) the reliable 10% limit when compared to those of $2a^+ \subset 1c$.²² To overcome this problem, K_a assessment was carried out by means of a competition experiment¹⁶ by mixing (in $CDCl_3$) 1 equiv of $2a^+TFPB^-$ with a 1:1 mixture of calix[5]arene $1c$ and calix[6]arene $3b$,^{11a, 22} after 30 min mixing, calix[6]-pseudorotaxane $2a^+ \subset 3b$ was preferentially formed over the calix[5]-pseudorotaxane one in a 4:1 ratio and with a total percentage of formation of 90% (Figure 4b). However, after equilibration at 298 K for 18 h, this preference was reversed and thus $2a^+ \subset 1c$ ultimately formed in a 9.5:0.5 ratio over $2a^+ \subset 3b$ (Figure 4c).

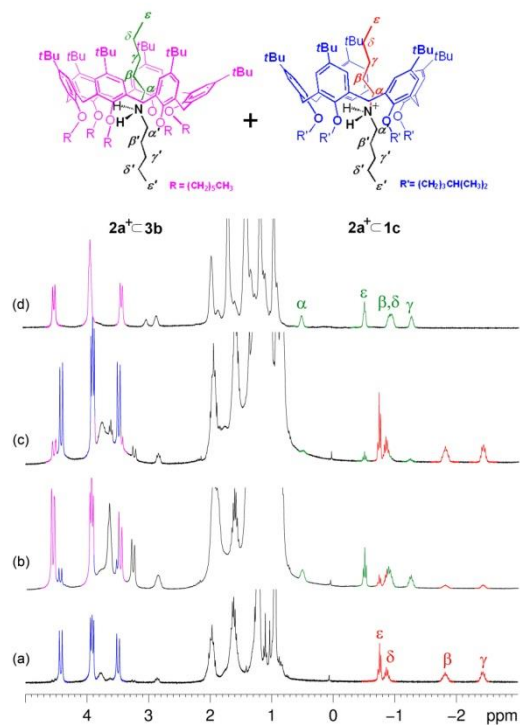


Figure 4. High-field regions of the 1H NMR spectra (300 MHz, $CDCl_3$, 298 K) of: (a) an equimolar solution (4.5 mM) of $1c$ and $2a^+TFPB^-$ after equilibration for 18 h at rt; (b) an equimolar solution (4.5 mM) of $2a^+TFPB^-$, $1c$ and $3b$ after 30 min from mixing; (c) an equimolar solution (4.5 mM) of $2a^+TFPB^-$, $1c$ and $3b$ after equilibration for 18 h at rt; (d) an equimolar solution (4.5 mM) of $3b$ and $2a^+TFPB^-$ after mixing.

These results indicate that the threading of the 24-membered calix[6]arene macrocycle –owing to its larger annulus– is kinetically faster than that of the 20-membered calix[5]arene one. Conversely, the $2\mathbf{a}^+\subset\mathbf{1c}$ pseudorotaxane displays greater thermodynamic stability. From the above-mentioned competition experiment, an apparent association constant of $2.02\pm 0.2 \times 10^5 \text{ M}^{-1}$ was calculated, a value significantly higher than that observed for the corresponding pseudorotaxane $2\mathbf{a}^+\subset\mathbf{1b}$ ($460\pm 50 \text{ M}^{-1}$).

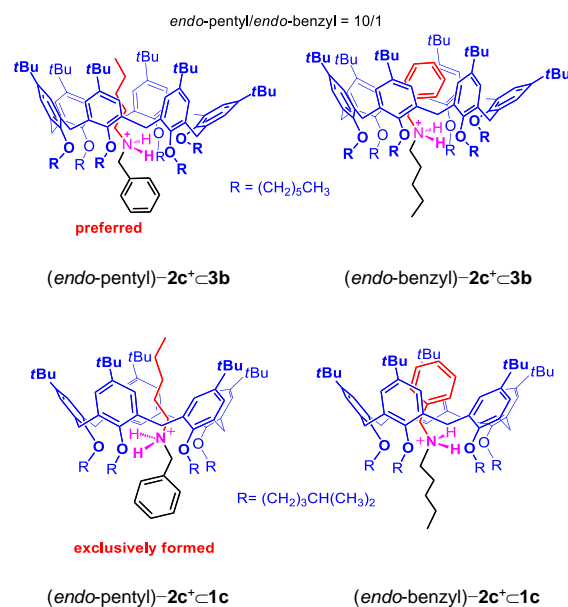


Figure 5. *Endo-pentyl/endo-benzyl* pseudorotaxane stereoisomers, obtainable by directional threading of the pentylbenzylammonium axle through the calix[6]arene and calix[5]arene wheels.

The above-described results clearly show that the narrow-rim substituents affect both the thermodynamic and kinetic properties of the calix[5]arene threading by dialkylammonium axles. To test the influence of the wide-rim substituents on the threading of the calix[5]arene wheel, we analyzed the ^1H NMR spectrum (CDCl_3) of a 1:1 mixture of $2\mathbf{a}^+\text{TFPB}^-$ and calix[5]arene $\mathbf{1d}$,¹⁶ bearing methyl groups at the wide rim. Consistent with the case of $\mathbf{1b}$, because of a fast *cone-to-cone* interconversion (via OMe passage through the annulus) after equilibration at 348 K for 96 h, only 4% of pseudorotaxane $2\mathbf{a}^+\subset\mathbf{1d}$ was detected.

Interestingly, no hint of threading was observed when $2\mathbf{a}^+\text{TFPB}^-$ was added to a CDCl_3 solution of penta-*O*-methyl-*p*-H-calix[5]arene derivative $1\mathbf{e}$.²³ Thus, these results unambiguously indicate that the presence of *tert*-butyl groups at the wide rim of a calix[5]arene macrocycle is mandatory for the formation of dialkylammonium/calix[5]arene pseudorotaxanes. *tert*-Butyl groups not only ensure preorganization of the calixarene cavity but, according to DFT data²⁴ gathered in the case of $2\mathbf{a}^+\text{c}1\mathbf{b}$, most likely contribute additional stabilization of the pseudorotaxane structure via van der Waals interactions with the alkyl chains of the axle (Figure 2).

Threading studies with the dibenzylammonium tetrakis[3,5-bis(trifluoromethyl)phenyl]borate ($2\mathbf{b}^+\text{TFPB}^-$) axle. The next question to answer was whether the 20-membered calix[5]arene-wheel is large enough to be threaded by a dibenzylammonium axle ($2\mathbf{b}^+$). Contrary to the calix[6]arene cases,^{11a} no hint of threading was observed upon addition of the $2\mathbf{b}^+\text{TFPB}^-$ salt to a CDCl_3 solution of any of the calix[5]arene derivatives $1\mathbf{b}$ – $1\mathbf{e}$. Analogous results were observed when, both a CDCl_3 and a 1,1,2,2-tetrachloroethane-*d*₂ (TCDE) solution of $2\mathbf{b}^+\text{TFPB}^-$ and $1\mathbf{c}$ (or $1\mathbf{b}$)¹⁶ were heated to 323 and 373 K, respectively for 7 days. On the other hand, when an excess of $\text{PhCH}_2\text{NH}_3^+\text{TFPB}^-$ salt was equilibrated with $1\mathbf{c}$ in CDCl_3 at 323 K for 24 h, the *endo*-cavity complex $\text{PhCH}_2\text{NH}_3^+\text{c}1\mathbf{c}$ was quantitatively formed.¹⁶ These combined data clearly indicate that the cavity of the *p-tert*-butylcalix[5]arene is wide enough to host a benzyl moiety while the diameter of the annulus^{21b, 25} is too narrow to allow its passage. It follows that the threading of a benzyl moiety through a calixarene wheel requires at least a 24-membered macroring (*e.g.*, a calix[6]arene).¹¹

Threading studies with the nonsymmetrical *n*-pentylbenzylammonium tetrakis[3,5-bis(trifluoromethyl)phenyl]borate ($2\mathbf{c}^+\text{TFPB}^-$) axle. The threading of asymmetric alkylbenzylammonium axles (*e.g.*, $2\mathbf{c}^+$) through calix[*n*]arene wheels of suitable size does in principle lead to the formation of two pseudorotaxane stereoisomers, namely the *endo*-alkyl and *endo*-benzyl ones (Figure 5).^{11a}

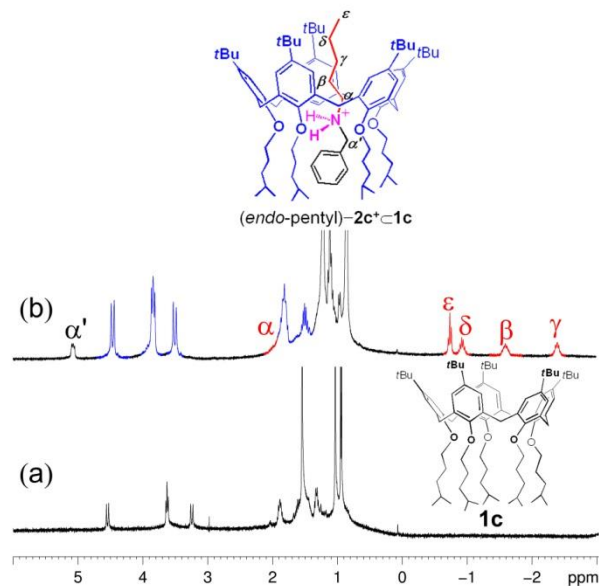


Figure 6. High-field regions of the ^1H NMR spectra (300 MHz, CDCl_3 , 298 K) of: (a) **1c**, (b) an equimolar solution (4.5 mM) of **1c** and **2c** $^+$ TFPB $^-$ after 18 h at rt.

In the case of calix[6]- and calix[8]arene wheels Errore. Il segnalibro non è definito.a.Errore. Il segnalibro non è definito.a we have consistently confirmed the so-called “*endo*-alkyl rule”²⁶ by which the *endo*-alkyl stereoisomer is preferentially formed (Figure 5).^{11a} Therefore, it was of some interest to verify if the *endo*-alkyl rule also applies to the case of calix[5]arene-wheels.

^1H NMR threading studies of **1c** with **2c** $^+$ TFPB $^-$ (Figure 6) clearly show highfield shifts (in the –0.80/–2.50 ppm region) characteristic^{11a} of the formation of the (*endo*-alkyl)–**2c** $^+$ –**1c** pseudorotaxane stereoisomer. On the other hand, the absence of shielded aromatic resonances in the $\delta = 4\text{--}6$ ppm region^{11a} is clear-cut proof that the *endo*-benzyl isomer is not formed (Figure 6b) thus confirming the inclusion of the alkyl moiety (*endo*-alkyl rule)²⁶ also in the cases of calix[5]arenes. Taking into account the fact that the benzyl moiety is too large to pass through the calix[5]arene annulus, it follows that the (*endo*-alkyl)–**2c** $^+$ –**1c** stereoisomer is toposelectively formed as a result of the passage of the alkyl group of **2c** $^+$ through the narrow rim of **1c** (Figure 8). To the best of our knowledge, this is the first example of topologically-controlled unidirectional threading through one of the two rims of a calixarene-wheel.²⁷

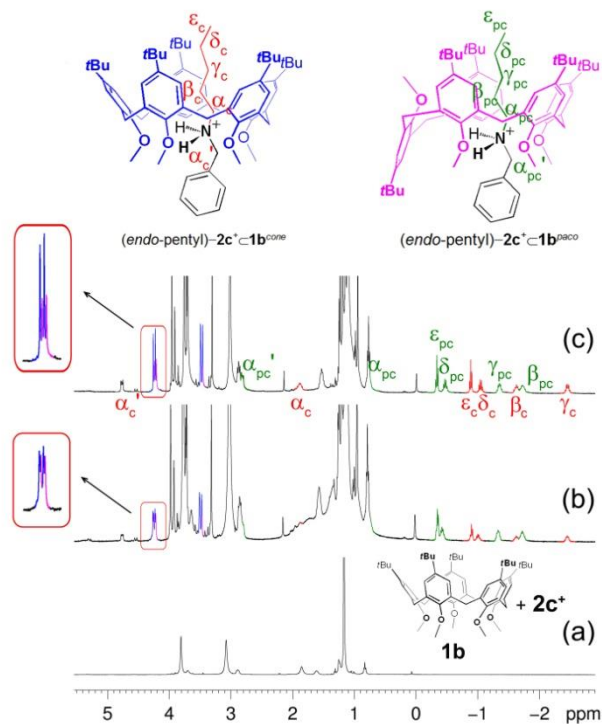


Figure 7. High-field regions of the ^1H NMR spectra (400 MHz, CDCl_3) of: (a) an equimolar solution (4.5 mM) of **1b** and $2\text{c}^+\text{TFPB}^-$ immediately after mixing; (b) an equimolar solution (4.5 mM) of **1b** and $2\text{c}^+\text{TFPB}^-$ after 12 h at rt; (c) an equimolar solution (4.5 mM) of **1b** and $2\text{c}^+\text{TFPB}^-$ after 46 h at 323 K.

The threading capability of the $2\text{c}^+\text{TFPB}^-$ axle was then tested in the presence of the conformationally mobile penta-*O*-methyl-*p*-*tert*-butylcalix[5]arene **1b**. After 12 h equilibration at rt, combined 1D (Figure 7b) and 2D NMR studies (COSY-45 and HSQC spectra¹⁶) clearly showed the presence of two pseudorotaxane structures, the first one $(\text{endo-pentyl})-2\text{c}^+\subset\mathbf{1b}^{\text{cone}}$, in which the dialkylammonium axle is threaded through a calix[5]arene-wheel adopting a *cone* conformation (red signals in Figure 7b), and the second one $(\text{endo-pentyl})-2\text{c}^+\subset\mathbf{1b}^{\text{paco}}$, in which the axle is seen inside a calix[5]arene wheel in a *partial-cone* (*paco*) conformation (green signals in Figure 7b).

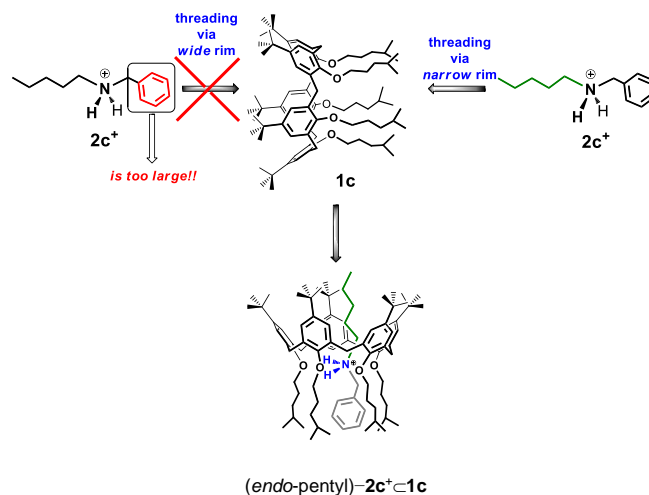


Figure 8. Unidirectional threading mode of $2\mathbf{c}^+$ through the narrow rim of $1\mathbf{c}$.

Careful integration of the pertinent signals belonging to the two pseudorotaxanes (after equilibration for 12 h at 298 K; Figure 7b), showed that the $(endo-pentyl)-2\mathbf{c}^+@1\mathbf{b}^{paco}$ was preferentially formed over the $(endo-pentyl)-2\mathbf{c}^+@1\mathbf{b}^{cone}$ in a 6:4 ratio.

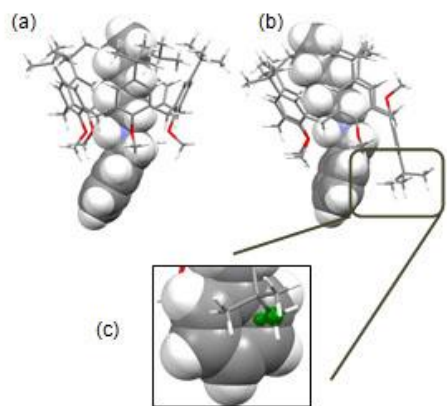


Figure 9. Optimized structures at the M06/6-31+G(d,p) level of theory of: (a) pseudorotaxane $2\mathbf{c}^+@1\mathbf{b}^{cone}$; (b) $2\mathbf{c}^+@1\mathbf{b}^{paco}$ and (c) inset of the C–H \cdots π (C–H \cdots $\pi^{centroid}$ distance = 2.71 Å) interaction between the *tert*-butyl group of $1\mathbf{b}$ and the “inverted” aromatic ring of $2\mathbf{c}^+$ in the $2\mathbf{c}^+@1\mathbf{b}^{paco}$ pseudorotaxane.

Conversely, a 4.5:5.5 (*endo*-pentyl)-**2c**⁺⊂**1b**^{paco}/*endo*-pentyl)-**2c**⁺⊂**1b**^{cone} ratio was detected upon equilibration of **1b** and **2c**⁺ for 46 h at 323 K. Interestingly, in both instances the absence of resonances in the diagnostic $\delta = 4\text{--}6$ ppm region of the ¹H NMR spectrum was judged to be a clear indication that the (*endo*-benzyl)-**2c**⁺⊂**1b** stereoisomer was not formed. A quantitative ¹H NMR analysis²² of a 1:1 mixture of **1b** and **2c**⁺ in CDCl₃, using 1,1,2,2-tetrachloroethane as an internal standard, led to apparent association constants of 205±18 and 180±15 M⁻¹ for the (*endo*-pentyl)-**2c**⁺⊂**1b**^{cone} and (*endo*-pentyl)-**2c**⁺⊂**1b**^{paco} complexes, respectively.

The DFT-optimized structures of the (*endo*-pentyl)-**2c**⁺⊂**1b**^{cone} and (*endo*-pentyl)-**2c**⁺⊂**1b**^{paco} pseudorotaxanes (Figure 9), at the M06/6-31+G(d,p) level of theory, indicate the formation of hydrogen bonds between the ammonium group of **2c**⁺ and the phenolic oxygen atoms of **1b**. In addition, in the case of the (*endo*-pentyl)-**2c**⁺⊂**1b**^{paco} structure, calculations suggest the presence of a C–H⋯ π interaction (Figure 9c) between the *tert*-butyl group of **1b** and an aromatic ring of **2c**⁺, with a C–H⋯ π^{centroid} distance of 2.71 Å. Close inspection of the DFT-optimized (*endo*-alkyl)-**2c**⁺⊂**1b**^{paco} structure reveals the presence of four C–H⋯ π interactions between the *endo*-pentyl chain and the aromatic rings of **1b** (average C–H⋯ π^{centroid} distance = 2.56 Å) likely responsible for the stabilization of the (*endo*-alkyl)-**2c**⁺⊂**1b**^{paco} pseudorotaxane complex.

Conclusions

In conclusion, we have shown that the *through-the-annulus* threading of 20-membered calix[5]arene macrocycles by dialkylammonium axles efficiently occurs when the latter are coupled to the loosely coordinating superweak TFPB⁻ anion. In more detail our data show that:

a) the greater the preorganization of a calix[5]arene, the greater the thermodynamic stability of the corresponding pseudorotaxane and the faster the kinetic of threading;

b) in comparison with calix[6]arene macrocycles, the threading of calix[5]arenes is kinetically slower, because of the narrower annulus; on the other hand, the resulting pseudo[2]rotaxanes display greater

thermodynamic stability as the result of a higher degree of preorganization of the 20-membered macroring;

c) the presence of *tert*-butyl groups on a calix[5]arene not only preorganizes the macrocycle –by avoiding the wide-rim *through-the-annulus* passage– but likely stabilizes the pseudorotaxane complex formed as a result of van der Waals interactions with the dialkylammonium axle;

d) the phenyl group of a benzylammonium axle is too large to thread the 20-membered calix[5]arene annulus;

e) by analogy with the larger calix[6–8]arenes, the threading of the calix[5]arene wheel with alkylbenzylammonium axles follows the “*endo*-alkyl rule”.

f) unprecedentedly, the toposelective formation of (*endo*-alkyl)–**2c**⁺⊂**1b**^{cone} and (*endo*-alkyl)–**2c**⁺⊂**1b**^{praco} pseudorotaxanes occurs via unidirectional axle threading (from the narrow-rim side) of the calix[5]arene wheel.

We believe that the present data are of considerable interest in the field of interpenetrated/interlocked structures and we are currently looking at the design of specific calix[5]arene-based rotaxane/catenane architectures.

Experimental Section

General Information.

Derivatives **2a–c**⁺, ¹¹ **1b**, ¹⁸ **1c**, ^{21a} and **1e** ²³ were synthesized according to literature procedures. ¹H NMR spectra were recorded at 298 K in CDCl₃ (at 300, 400 or 600 MHz), using the residual solvent signal as the internal standard. COSY-45 spectra were taken using a relaxation delay of 2 s with 30 scans and 170 increments of 2048 points each. HSQC spectra were performed with the gradient selection, sensitivity enhancement, and phase-sensitive mode using an Echo/Antiecho-TPPI procedure. Typically, 20 scans with 113 increments of 2048 points each were acquired.

5,11,17,23,29-Pentamethyl-31,32,33,34,35-pentamethoxycalix[5]arene (1d). A stirred mixture of **1f**²⁸ (0.85 g, 1.41 mmol), CH₃I (3.0 g, 21.15 mmol) and K₂CO₃ (2.92 g, 21.15 mmol) in anhydrous CH₃CN (30 mL) was refluxed for 24 h under N₂. The solvent was evaporated under reduced pressure, and the residue was partitioned between chloroform (30 mL) and aqueous HCl (1 M, 30 mL). The organic layer was separated, washed with water (2 × 30 mL) and dried (MgSO₄). Evaporation of the solvent left a crude solid that was recrystallized from CH₃CN/CHCl₃ to afford **1d** as white solid (0.64 g, 68%). M.p. >180 °C dec.; ¹H NMR (600 MHz, CDCl₃) δ 2.15 (s, CH₃, 15 H), 3.18 (s, OCH₃, 15 H), 3.79 (s, ArCH₂Ar, 10 H) and 6.77 (s, ArH, 10 H) ppm; ¹³C NMR (150 MHz, CDCl₃) δ 21.1, 31.1, 60.8, 129.7, 132.4, 134.5 and 154.7 ppm; elemental analysis calcd (%) for C₄₅H₅₀O₅: C 80.56, H 7.51; found: C 80.34, H 7.69.

General procedure for the preparation of pseudorotaxane complexes.

Calix[5]arene derivatives (2.25×10⁻³ mmol) and the appropriate dialkylammonium TFPB salts **2a-c**⁺ (2.25×10⁻³ mmol) were dissolved in CDCl₃ (0.5 mL). The solution was sonicated for 15 min at room temperature and then transferred into a NMR tube for 1D and 2D NMR spectra acquisition.

Acknowledgment. We thank the MIUR (PRIN 20109Z2XRJ_006) for financial support and the Centro di Tecnologie Integrate per la Salute (CITIS, Project PONA3_00138), Università di Salerno, for the 600 MHz NMR facilities. Thanks are due to Dr. Patrizia Iannece and to Dr. Patrizia Oliva (Dipartimento di Chimica e Biologia, Università di Salerno) for ESI-MS and NMR spectral measurements, respectively.

Supporting Information: 1D and 2D NMR spectra of pseudorotaxanes, determination of stability constants, details on C–H···π contacts in DFT-optimized structure of **2a**⁺·**1b** pseudorotaxane, atomic coordinates of DFT-optimized pseudorotaxane structures, this materials is available free of charge via the Internet at <http://pubs.acs.org>.

REFERENCES

1. (a) Amabilino, D. B.; Stoddart, J. F. *Chem. Rev.*, **1995**, *95*, 2725-2728. (b) Sauvage, J. P., Dietrich-Buchecker C., (Eds), *Molecular Catenanes, Rotaxanes and Knots: A Journey Through the World of Molecular Topology*, Wiley-VCH, Weinheim, 1999. (c) Xue, M.; Yang, Y.; Chi, X.; Yan, X.; Huang, F. *Chem. Rev.* **2015**, *115*, 7398–7501.
2. (a) Saha, S.; Stoddart, J. F. *Chem. Soc. Rev.* **2007**, *36*, 77-92. (b) Balzani, V., Credi, A., Venturi, M., (Eds), *Molecular devices and machines*, 2nd ed., Wiley- VCH, Weinheim, 2008. (c) Fahrenbach, A. C.; Bruns, C. J.; Cao, D.; Stoddart, J. F. *Acc. Chem. Res.* **2012**, *45*, 1581–1592. (d) Erbas-Cakmak, S.; Leigh, D. A.; MacTernan, C. T.; Nussbaumer, A. L. *Chem. Rev.* **2015**, *115*, 10081–10206. (e) Kay, E. R.; Leigh, D. A. *Angew. Chem. Int. Ed. Engl.* **2015**, *54*, 10080–10088.
3. (a) Blanco, V.; Carlone, A.; Hänni, K. D.; Leigh, D. A.; Lewandoski, B. *Angew. Chem. Int. Ed. Engl.* **2012**, *51*, 5166–5169. (b) Blanco, V.; Leigh, D. A.; Marcos, V.; Morales-Serna, J. A.; Nussbaumer, A. L. *J. Am. Chem. Soc.* **2014**, *136*, 4905–4908. (c) Leigh, D. A.; Marcos, V.; Wilson, M. R. *ACS Catal.* **2014**, *4*, 4490–4497. (d) Blanco, V.; Leigh, D. A.; Lewandowska, U.; Lewandoski, B.; Marcos, V. *J. Am. Chem. Soc.* **2014**, *136*, 15775–15790.
4. Ashton, P. R. ; Campbell, P. J.; Chrystal, E. J. T.; Glink, P. T.; Menzer, S.; Philp, D.; Spencer, N.; Stoddart, J. F.; Tasker, P. A.; Williams, D. J. *Angew. Chem. Int. Ed. Engl.* **1995**, *34*, 1865–1869.
5. Harada, A.; Takashima, Y.; Nakahata, M. *Acc. Chem. Res.* **2014**, *47*, 2128–2140.
6. (a) Lee, J. W.; Samal, S.; Selvapalam, N.; Kim, H. J.; Kim, K. *Acc. Chem. Res.* **2003**, *36*, 621–630. (b) Lagona, J.; Mukhopadhyay, P.; Chakrabarti, S.; Isaacs, L. *Angew. Chem. Int. Ed.* **2005**, *44*, 4844–4870.

7. (a) Leigh, D. A.; Wong, J. K. Y.; Dehez, F.; Zerbetto, F. *Nature* **2003**, *424*, 174–179. (b) Hernandez, J. V.; Kay, E. R.; Leigh, D. A. *Science* **2004**, *306*, 1532–1537. (c) Leigh, D. A.; Lusby, P. J.; Slawin, A. M. Z.; Walker D. B. *Chem. Comm.* **2012**, *50*, 4476–4787.
8. (a) Arduini, A.; Orlandini, G.; Secchi, A.; Credi, A.; Silvi, S.; Venturi M. in *Calixarenes and Beyond* (Eds.: P. Neri, J. L. Sessler, M.-X. Wang), Elsevier, Oxford, 2016, pp.761–781. (b) Gaeta, C.; Talotta, C.; De Rosa, M.; Soriente, A.; Neri P. in *Calixarenes and Beyond* (Eds.: P. Neri, J. L. Sessler, M.-X. Wang), Elsevier, Oxford, 2016, pp.783–809.
9. (a) Ogoshi, T.; Kanai, S.; Fujinami, S.; Yamagishi, T.; Nakamoto, Y. *J. Am. Chem. Soc.* **2008**, *130*, 5022–5023. (b) Xiong, S.; Zhnag, X.; Meng, L.-B.; Jiang, J.; Lin, C.; Wang, L. *Chem. Commun.* **2015**, *51*, 6504–6507. (c) Strutt, N.; Forgan, R. S.; Spruell, J. M.; Botros, Y. Y.; Stoddart J. F. *J. Am. Chem. Soc.* **2011**, *133*, 5668–5671.
10. (a) Arduini, A.; Ferdani, R.; Pochini, A.; Secchi, A.; Ugozzoli, F. *Angew. Chem.* **2000**, *112*, 3595–3598; *Angew. Chem. Int. Ed.* **2000**, *39*, 3453–3456. (b) Arduini, A.; Bussolati, R.; Credi, A.; Secchi, A.; Silvi, S.; Semeraro, M.; Venturi, M. *J. Am. Chem. Soc.* **2013**, *135*, 9924–9930 and references therein.
11. (a) Gaeta, C.; Troisi, F.; Neri, P. *Org. Lett.* **2010**, *12*, 2092–2095. (b) Talotta, C.; Gaeta, C.; Neri, P. *Org. Lett.* **2012**, *14*, 3104–3107.
12. (a) Strauss, S. H. *Chem Rev.* **1993**, *93*, 927–942. (b) Nishida, H.; Takada, N.; Yoshimura, M.; Sonoda, T.; Kobayashi, H. *Bull. Chem. Soc. Jpn.* **1984**, *57*, 2600–2604. For recent examples on the use of TFPB superweak anion in supramolecular chemistry, see: (c) Li, C.; Shu, X.; Li, J.; Fan, J.; Chen, Z.; Weng, L.; Jia, X. *Org. Lett.* **2012**, *14*, 4126–4129. (d) Blight, B. A.; Camara-Campos, A.; Djurdjevic, S.; Kaller, M.; Leigh, D. A.; McMillan, F. M.; Mc Nab, H.; Slawin, A. M. *J. Am. Chem. Soc.* **2009**, *131*, 14116–14122. (e) Hou, H.; Leung, K. C.-F.; Lanari, D.; Nelson, A.; Stoddart, J. F.; Grubbs, R. H. *J. Am. Chem. Soc.* **2006**, *128*, 13358–

13359. For a review on counterion effects in supramolecular chemistry, see: (f) Gasa, T. B.; Valente, C.; Stoddart, J. F. *Chem. Soc. Rev.* **2011**, *40*, 57–78.
13. (a) Gaeta, C.; Talotta, C.; Margarucci, L.; Casapullo, A.; Neri, P. *J. Org. Chem.* **2013**, *78*, 7627–7638. (b) Talotta, C.; Gaeta, C.; Neri, P. *J. Org. Chem.* **2014**, *79*, 9842–9846. (c) De Rosa, M.; Talotta, C.; Soriente, A. *Lett. Org. Chem.* **2009**, *6*, 301–305. (d) Talotta, C.; Gaeta, C.; De Rosa, M.; Ascenso, J. R.; Marcos, P. M.; Neri, P. *Eur. J. Org. Chem.* **2016**, *1*, 158–167. (e) Gaeta, C.; Talotta, C.; Farina, F.; Camalli, M.; Campi, G.; Neri, P. *Chem. Eur. J.* **2012**, *18*, 1219–1230.
14. Barrett, G.; McKervey, M. A.; Malone, J. F.; Walker, A.; Arnaud-Neu, F.; Guerra, L.; Schwing-Weill, M.-J.; Gutsche, C. D.; Stewart, D. R. *J. Chem. Soc. Perkin Trans. 2* **1993**, 1475–1479.
15. Gattuso, G.; Notti, A.; Parisi, M. F.; Pisagatti, I.; Amato, M. E.; Pappalardo, A.; Pappalardo, S. *Chem. Eur. J.* **2010**, *16*, 2381–2385.
16. See the Supporting Information for further details.
17. (a) Li, C.; Shu, X.; Li, J.; Fan, J.; Chen, Z.; Weng, L.; Jia, X. *Org. Lett.* **2012**, *14*, 4126–4129. (b) Chen, N.-C.; Chuang, C.-J.; Wang, L.-Y.; Lai, C.-C.; Chiu, S.-H. *Chem. Eur. J.* **2012**, *18*, 1896–1900.
18. Stewart, D. R.; Krawiec, M.; Kashyap, R. T.; Watson, W. H.; Gutsche, C. D. *J. Am. Chem. Soc.* **1995**, *117*, 586–601.
19. The *through-the-annulus* passage of the 4-*t*Bu-2,6-phenylene moiety is known to be hampered in the case of *p-tert*-butylcalix[5]arene penta-*O*-ethers. See: Ferguson, G.; Notti, A.; Pappalardo, S.; Parisi, M. F.; Spek, A. L. *Tetrahedron Lett.* **1998**, *39*, 1965–1968.
20. Including the sharp singlet at $\delta = 3.82$ ppm assigned to the bridging methylene hydrogen atoms.

21. (a) Arnaud-Neu, F.; Fuangswasdi, S.; Notti, A.; Pappalardo, S.; Parisi, M. F. *Angew. Chem.* **1998**, *110*, 120–122; *Angew. Chem. Int. Ed.* **1998**, *37*, 112–114. (b) Gattuso, G.; Notti, A.; Pappalardo, S.; Parisi, M. F.; Pilati, T.; Resnati, G.; Terraneo, G. *CrystEngComm* **2009**, *11*, 1204–1206.
22. (a) Hirose, K. *J. Inclusion Phenom. Macrocyclic Chem.* **2001**, *39*, 193–209. (b) Hirose, K. in *Analytical Methods in Supramolecular Chemistry*, (Ed: C. A. Schalley), Wiley-VCH, Weinheim, 2007, Chapter 2, 17–54. (c) Braun, S., Kalinowsky, H.-O., Berger, S., Eds., *150 and More Basic NMR experiments: A Practical Course*, Wiley-VCH, Weinheim, 1996, 232–233.
23. Wang, J.; Gutsche C. D. *J. Org. Chem.* **2002**, *67*, 4423–4429.
24. Close inspection of the $2\mathbf{a}^+\cdots\mathbf{1b}$ DFT-structure in Figure 2, reveals the presence of weak C-H $\cdots\pi$ interactions between the *endo*-pentyl chain of axle $2\mathbf{a}^+$ and the aromatic walls of $\mathbf{1b}$ with an average C-H $\cdots\pi^{centroid}$ distance of 3.30 Å. In addition, close contacts were revealed between the *tert*-butyl groups of $\mathbf{1b}$ and the δ -methylene and ε -methyl groups with an average C \cdots C distance of 3.99 Å.
25. For a selection of X-ray studies on calix[5]arenes see: (a) Buscemi, S.; Pace, A.; Piccionello, A. P.; Pappalardo, S.; Garozzo, D.; Pilati, T.; Gattuso, G.; Pappalardo, A.; Pisagatti, I.; Parisi, M. F. *Tetrahedron Lett.* **2006**, *47*, 9049–9052. (b) Capici, C.; Gattuso, G.; Notti, A.; Parisi, M. F.; Pappalardo, S.; Brancatelli, G.; Geremia, S. *J. Org. Chem.* **2012**, *77*, 9668–9675. (c) Brancatelli, G.; Pappalardo, S.; Gattuso, G.; Notti, A.; Pisagatti, I.; Parisi, M. F.; Geremia, S. *CrystEngComm* **2014**, *16*, 89–93. (d) Brancatelli, G.; Gattuso, G.; Geremia, S.; Notti, A.; Pappalardo, S.; Parisi, M. F., Pisagatti, I. *Org. Lett.* **2014**, *16*, 2354–2357. (e) Brancatelli, G.; Gattuso, G.; Geremia, S.; Manganaro, N.; Notti, A.; Pappalardo, S.; Parisi, M. F.; Pisagatti, I. *CrystEngComm* **2016**, *17*, 5012–5016.

26. Ciao, R.; Talotta, C.; Gaeta, C.; Margarucci, L.; Casapullo, A.; Neri, P. *Org. Lett.* **2013**, *15*, 5694–5697.
27. For additional studies regarding the directionality of the threading motion with calixarene-wheels, see ref 10b.
28. (a) T. Haino, M. Yanase, Y. Fukazawa *Tetrahedron Lett.* **1997**, *38*, 3739-3742. (b) T. Haino, M. Yanase, Y. Fukazawa *Angew. Chem., Int. Ed.* **1997**, *36*, 259-260. (c) C. Gargiuli, G. Gattuso, A. Notti, S. Pappalardo, M. F. Parisi *Tetrahedron Lett.* **2011**, *52*, 7116-7120.